

1 **Mapping CH₄:CO₂ ratios in Los Angeles with CLARS-FTS**
2 **from Mount Wilson, California**

3

4 **K. W. Wong¹, D. Fu¹, T. J. Pongetti¹, S. Newman², E. A. Kort⁴, R. Duren¹, Y.-K. Hsu³,**
5 **C. E. Miller¹, Y. L. Yung² and S. P. Sander¹**

6

7 [1] {NASA Jet Propulsion Laboratory, Pasadena, California, United States}

8 [2] {California Institute of Technology, Pasadena, California, United States}

9 [3] {California Air Resources Board, Sacramento, California, United States}

10 [4] {University of Michigan, Ann Arbor, Michigan, United States}

11 Correspondence to: K. W. Wong (clare.wong@jpl.nasa.gov)

12

13 Copyright 2014. California Institute of Technology. Government sponsorship acknowledged.

14

15 **Abstract**

16 The Los Angeles megacity, which is home to more than 40% of the population in California, is
17 the second largest megacity in the United States and an intense source of anthropogenic
18 greenhouse gases (GHGs). Quantifying GHG emissions from the megacity and monitoring their
19 spatiotemporal trends are essential to be able to understand the effectiveness of emission control
20 policies. Here we measure carbon dioxide (CO₂) and methane (CH₄) across the Los Angeles
21 megacity using a novel approach – ground-based remote sensing from a mountaintop site. A
22 Fourier Transform Spectrometer (FTS) with agile pointing optics, located on Mount Wilson at
23 1.67 km above sea level, measures reflected near infrared sunlight from 29 different surface
24 targets on Mount Wilson and in the Los Angeles megacity to retrieve the slant column
25 abundances of CO₂, CH₄ and other trace gases above and below Mount Wilson. This technique

1 provides persistent space and time resolved observations of path-averaged dry-air GHG
2 concentrations, XGHG, in the Los Angeles megacity and simulates observations from a
3 geostationary satellite. In this study, we combined high sensitivity measurements from the FTS
4 and the panorama from Mount Wilson to characterize anthropogenic CH₄ emissions in the
5 megacity using tracer:tracer correlations. During the period between September 2011 and
6 October 2013, the observed XCH₄:XCO₂ excess ratio, assigned to anthropogenic activities,
7 varied from 5.4 to 7.3 ppb CH₄(ppm CO₂)⁻¹, with an average of 6.4 ± 0.5 ppb CH₄ (ppm CO₂)⁻¹
8 compared to the value of 4.6 ± 0.9 ppb CH₄ (ppm CO₂)⁻¹ expected from the California Air
9 Resources Board (CARB) bottom-up emission inventory. Persistent elevated XCH₄:XCO₂ excess
10 ratios were observed in Pasadena and in the eastern Los Angeles megacity. Using the FTS
11 observations on Mount Wilson and the bottom-up CO₂ emission inventory, we derived a top-
12 down CH₄ emission of 0.39 ± 0.06 Tg CH₄ year⁻¹ in the Los Angeles megacity. This is 18–61 %
13 larger than the state government’s bottom-up CH₄ emission inventory and consistent with
14 previous studies.

15

16 **1 Introduction**

17 The Los Angeles megacity – a sprawling urban expanse of ~100 km x 100 km and 15 million
18 people – covers only ~4% of California’s land area but is home to more than 43% of its
19 population and dominates the state’s anthropogenic greenhouse gas (GHG) emissions. By
20 treating the megacity as an effective ‘point source’, we can quantify trends in this critical
21 component of the state’s GHG emissions and support California’s goal of reducing GHG
22 emissions to the 1990 level by 2020 mandated by the state’s The Global Warming Solutions Act
23 of 2006 (AB32).

24 Emissions of carbon dioxide (CO₂) and methane (CH₄) in the Los Angeles megacity originate
25 largely from different economic sectors and are expected to have distinctly different spatial and
26 temporal patterns. Anthropogenic CO₂ is derived mainly from motor vehicle exhaust
27 (Transportation), exhibiting strong diurnal variability and weak seasonal variability, and from
28 natural gas fueled power plants (Power) with a few large stationary emitters and significant
29 seasonal variability. Overall CO₂ emissions for transportation and power plants are known to

1 within $\pm 10\%$ from fuel usage and emission factors (de la Rue du Can et al., 2008). On the other
2 hand, the CH₄ emissions budget is highly uncertain and contains significant but poorly quantified
3 emissions from a variety of sources such as landfills and wastewater treatment plants (Waste), oil
4 and gas production, storage and delivery infrastructure (Power and Residential), dairy farms
5 (Agriculture) and geologic seeps (Geology). Recent studies estimating CH₄ emissions from
6 atmospheric observations have shown that the bottom-up total CH₄ emissions inventory in the
7 Los Angeles megacity have uncertainties of 30% to >100% (Wunch et al., 2009; Hsu et al.,
8 2010; Wennberg et al., 2012; Jeong et al., 2013; Peischl et al., 2013). Atmospheric observations
9 may be used to characterize spatial and temporal patterns in CO₂ and CH₄ within the Los
10 Angeles megacity and to provide initial estimates of sectoral emissions attribution.

11 Wunch et al. (2009) demonstrated the estimation of GHGs using the ground-based column
12 measurements acquired at a Total Carbon Column Observing Network (TCCON) station in
13 Pasadena, California, in the Los Angeles basin. Since column measurements are relatively
14 insensitive to boundary layer height variations and are less influenced by local surface sources
15 than ground in situ measurements, they should be more representative of the area. They reported
16 that the bottom-up CH₄ emissions for the Los Angeles megacity are less than half of the top-
17 down CH₄ emissions. The large uncertainty in the bottom-up CH₄ emission inventory in the Los
18 Angeles megacity has also been supported by the CH₄:CO₂ ratios observed by aircraft
19 campaigns, ARCTAS-CARB in 2008 and CalNex in 2010 (Wennberg et al., 2012; Peischl et al.,
20 2013), and in situ observations on Mount Wilson (Hsu et al., 2010).

21 Despite the potential of atmospheric observations to quantify the emissions of CH₄, CO₂ and
22 other GHGs in the Los Angeles megacity, they have certain limitations for tracking long-term
23 GHG emissions. Kort et al. (2013) showed that surface in situ observations from no single site
24 within or adjacent to the Los Angeles megacity accurately capture the emissions from the entire
25 region. Similarly, ground-based total column measurements from Pasadena also lack sensitivity
26 to emissions from across the entire region. Kort et al. (2013) concluded that the size and
27 complexity of the Los Angeles megacity urban dome requires a network of at least eight
28 strategically located continuous surface in situ observing sites to quantify and track GHG
29 emissions over time with $\sim 10\%$ uncertainty. However, this minimum network would have
30 limited capabilities to identify and isolate emissions from specific sectors and/or localized

1 sources. It is therefore necessary to develop a robust, long-term measurement solution, which
2 resolves emissions the Los Angeles megacity both spatially and temporally.

3 The present study reports GHG measurements of the Los Angeles megacity from an elevated
4 vantage, the California Laboratory for Atmospheric Remote Sensing (CLARS), located on Mt
5 Wilson 1670 m a.s.l. and overlooking the Los Angeles megacity (Fig. 1). We present column
6 averaged dry air mole fraction CO_2 (XCO_2) and CH_4 (XCH_4) measurements for 29 reflection
7 points distributed across Los Angeles. The measurements cover daytime hours for the two-year
8 period between 2011 and 2013. We determine the enhancements in XCH_4 and XCO_2 in the basin
9 compared to background levels, and use the spatial distribution of $\text{XCH}_4(\text{excess}):\text{XCO}_2(\text{excess})$
10 ratio to quantify emissions in the megacity. We compare our results to column, surface in situ
11 and aircraft in situ observations and compare our derived megacity CH_4 emissions estimates with
12 the results from previous studies.

13 CLARS provides a unique long-term record that simulates geostationary satellite observations
14 (GEO) for the Los Angeles basin. CLARS maps the diurnal variability of both XCO_2 and XCH_4
15 within the Los Angeles urban dome with hourly time scales. It has functioned operationally since
16 2011, and its sustained measurements are yielding insights into the scientific value of GEO GHG
17 monitoring, as well as helping to define GEO-based GHG measurement requirements. Existing
18 and future satellite instruments such as TES (AURA), TANSO-FTS (GOSAT), and OCO-2, all
19 sample from sun-synchronous low-earth orbits. These platforms sample globally, but return to
20 the same measurement point on the Earth infrequently, with repeat cycles ranging from days to
21 weeks. In contrast, GEO measurements, such as those from the proposed Geostationary Fourier
22 Transform Spectrometer (GEO-FTS), map the complete field of regard with high spatial
23 resolution (<10 km horizontal resolution) many times per day (Key et al., 2012). Measurements
24 from a mountaintop location, such as CLARS, provide similar spatial and temporal resolution as
25 GEO measurements but with a larger viewing zenith angle which enhances the optical path in the
26 planetary boundary layer. We also demonstrate simultaneous XCH_4 and XCO_2 measurements are
27 essential to quantify megacity GHG emissions and also provide critical information from which
28 to attribute emissions from different economic sectors.

29

30 **2 Measurement technique**

1 2.1 CLARS-FTS

2 A JPL-built Fourier Transform Spectrometer (FTS) has been deployed since 2010 at the CLARS
3 facility on Mount Wilson at an altitude of 1670 m a.s.l. overlooking the Los Angeles megacity
4 (Fig. 1). The FTS operates in two modes: the Spectralon Viewing Observations (SVO) and the
5 Los Angeles megacity Surveys (LABS). In the SVO mode, the FTS points at a Spectralon® plate
6 placed immediately below the FTS telescope to quantify the total column CO₂ and CH₄ above the
7 Los Angeles megacity (above 1670 m and the basin planetary boundary layer (PBL) height). The
8 SVO measurements represent approximately free tropospheric background levels. In the LABS
9 mode, the FTS points downward at 28 geographical points in the basin acquiring spectra from
10 reflected sunlight in the near-infrared region (Table 1). Our measurement technique from Mount
11 Wilson mimics satellite observations, which measure surface reflectance from space or
12 atmospheric absorptions of GHGs along the optical path – (1) from the sun to the surface and (2)
13 from the surface to the instrument. The locations of the reflection points are selected to provide
14 the best coverage of the megacity (Fig. 1). In addition, reflection points are chosen with uniform
15 surface albedo across the spectrometer field of view using a near infrared camera. Reflection
16 points sample from the San Bernardino Mountains in the east to the Pacific coast in the west, and
17 from the base of the San Gabriel Mountains in the north to Long Beach Harbor and Orange
18 County in the south. For a typical PBL height, the geometric slant paths within the PBL range
19 from ~4 km (Santa Anita Park) to ~39 km (Lake Mathews). The points in Table 1 are the
20 baseline raster pattern, but can be modified easily if desired. In the standard measurement cycle,
21 the FTS points at these 28 reflection points and performs four SVO measurements per cycle.
22 There are 5-8 measurement cycles per day depending on the time of the year.

23 The spectral resolution used in the CLARS-FTS measurement is 0.12 cm⁻¹, with an angular
24 radius of the field of view of 0.5 mrad. The footprints in the Los Angeles megacity are ellipses
25 with surface area ranging from 0.04 to 21.62 km² (Table 1). The pointing calibration procedure is
26 designed to maximize pointing accuracy (Fu et al., 2014). Pointing uncertainties are primarily
27 due to errors arising from gimbal tilt and minor position-dependent flexing of the pointing
28 system structure. After pointing calibration corrections are applied, the CLARS-FTS pointing
29 system has a total uncertainty of 0.17° deg (1 sigma) in azimuth, which is about 30% of the
30 CLARS-FTS field of view. This results in a ground distance error of about 60 m for a reflection

1 point located 20 km from Mount Wilson. Uncertainty is 0.045 deg (1 sigma) in elevation, that is,
2 8% of the CLARS-FTS field of view, resulting in a ground distance error of about 16 m for a
3 target that is 20 km from Mount Wilson. Details concerning the CLARS-FTS design, operation
4 and calibration are described in Fu et al. (2014).

5 **2.2 Data processing**

6 The CLARS interferogram processing program (CLARS-IPP) converts the recorded
7 interferograms into spectra. The CLARS-IPP also corrects for solar intensity variations and
8 phase error. 12 single scan spectra are co-added over a period of 3 minutes for each reflection
9 point to achieve a spectral signal-to-noise ratio (SNR) of $\sim 300:1$ for LABS measurements and \sim
10 $450:1$ for SVO measurements. The instrument line shape (ILS) of the CLARS-FTS is
11 characterized using an external lamp and an HCl gas cell. Our experiment works on a simple
12 Beer-Lambert principle where the number densities of CO_2 and CH_4 are proportional to the
13 optical depths measured for rotationally resolved near infrared absorption spectra. Slant column
14 density (SCD), the total number of absorbing molecule per unit area along the sun-Earth-
15 instrument optical path, is retrieved for CO_2 and CH_4 using a modified version of the GFIT
16 algorithm (Wunch et al., 2011; Fu et al., 2014). Descriptions of the CLARS-FTS data processing
17 and retrieval algorithm are included in Fu et al., 2014. In the present analysis, we retrieve CO_2
18 from bands at $1.6 \mu\text{m}$, CH_4 at $1.67 \mu\text{m}$, and O_2 at $1.27 \mu\text{m}$. The retrieved SCDs are converted to
19 slant column-averaged dry air mole fractions, XCO_2 and XCH_4 , by normalizing to SCD_{O_2}
20 (Equation 1).

$$21 \quad \text{XGHG} = \frac{\text{SCD}_{\text{GHG}}}{\text{SCD}_{\text{O}_2}} \times 0.2095 \quad (1)$$

22 This method has been shown to improve the precision of XCO_2 and XCH_4 retrievals since SCD_{O_2}
23 retrieval effectively cancels out first-order path length, instrumental, and retrieval algorithm
24 errors (Washenfelder and Wennberg, 2003; Washenfelder et al., 2006; Wunch et al., 2011; Fu et
25 al., 2014). Measurement precisions are 0.3 ppm for XCO_2 ($\sim 0.1\%$) and 2.5 ppb for XCH_4
26 ($\sim 0.1\%$) for the SVO measurements and 0.6 ppm for XCO_2 ($\sim 0.1\%$) and 4.7 ppb for XCH_4
27 ($\sim 0.2\%$) for the LABS measurements. Estimated measurement accuracies are $<3.1\%$ for XCO_2
28 and $<6.0\%$ for XCH_4 , driven mainly by uncertainties in laboratory spectra line parameters.

1 **2.3 Data filtering**

2 Poor air quality in Los Angeles causes visibility reduction due to aerosol scattering. While the
3 impact of aerosol scattering is significantly lower in the infrared than the visible and ultraviolet
4 spectral regions, CLARS-FTS trace gas retrievals can be affected by aerosols due to the long
5 optical path length in the boundary layer. In addition to aerosol, the Los Angeles megacity is
6 often affected by morning marine layer fog and low clouds, which influence the data quality.

7 Individual retrievals are analyzed with multiple post-processing filters to ensure data quality,
8 similar to the QA/QC filters adopted in the Atmospheric CO₂ observations from Space (ACOS) -
9 GOSAT data processing (O'Dell et al., 2012; Crisp et al. 2012; Mandrake et al., 2013). Table 2
10 summarizes the filtering criteria. Data with poor spectral fitting quality, such as with large solar
11 zenith angle (SZA), low SNR and/or large fitting residual root mean square errors (RMS), are
12 removed. Data are also screened for clouds and aerosols using the ratio of retrieved to geometric
13 oxygen SCDs as the criterion. The geometric oxygen SCD is calculated using surface pressure
14 from National Center for Environmental Prediction (NCEP) reanalysis data assuming hydrostatic
15 equilibrium, a constant oxygen dry-air volume mixing ratio of 0.2095 along the optical path and
16 no scattering or absorption occurs (Fu et al., 2014). Because oxygen is well mixed in the
17 atmosphere, deviations in the retrieved oxygen SCD from the geometric oxygen SCD indicate
18 variations of the light path due to clouds and/or aerosols, assuming deviations are larger than the
19 retrieval uncertainty, that is, <0.3% for SVO measurements and ~0.5% for LABS measurements
20 (errors represent precisions only). For high clouds, data are filtered out when the corresponding
21 SVO oxygen SCD ratio is less than 1 or greater than 1.1. For low clouds, data with retrieved
22 target oxygen SCD deviating more than 10% from the geometric value are removed. We use the
23 same criteria to take out data with heavy aerosol loading which leads to significant modification
24 in the light path. This filtering approach is equivalent to that used by ACOS, which compares the
25 retrieved surface pressure to reanalysis data (O'Dell et al., 2012). As a result of our data filters,
26 more data are removed for reflection points located further away from Mount Wilson since these
27 measurements have larger fractions of their optical paths in the PBL and are more likely to
28 encounter substantial scattering (Fig. 2).

29 Numerous studies have shown that aerosol scattering the atmosphere has an impact on the
30 retrieved trace gas mixing ratios from space-based observations in the near-infrared (Aben et al.,

1 2007; Yoshida et al., 2011; Crisp et al., 2012). Zhang et al. (2014) used a numerical two-stream
2 radiative transfer model (RTM) validated against the VLIDORT full-physics RTM (Spurr et al.,
3 2006) to estimate the expected biases in the retrieved values of XCO₂ and XCH₄ from CLARS
4 observations. The model was used to set the value for the CLARS aerosol filter criterion in terms
5 of the ratio of measured to geometric optical path length derived from the 1.27μm absorption
6 band of molecular oxygen (see section 4.1).

7

8 **3 Observations**

9 **3.1 Diurnal variations of XCO₂ and XCH₄: SVO vs. LABS**

10 Due to the difference in the measurement geometry between the SVO mode and the LABS
11 mode, the diurnal patterns of XCO₂ and XCH₄ differ significantly. Figure 3 shows an example of
12 the diurnal variations of raw and filtered XCO₂ and XCH₄ measurements for the SVO mode, and
13 the LABS west Pasadena and Santa Anita Park targets from ~8:30 to ~16:30 LT on seven
14 continuous days during the period of May 5-11, 2012. The SVO retrievals showed constant path-
15 averaged mixing ratios of about 390 ppm XCO₂ and 1700 ppb XCH₄ during this period. The
16 constant diurnal pattern was observed because the FTS is located most of the time above the
17 planetary boundary layer where sources are located (Newman et al., 2013). Therefore the SVO
18 measurements do not capture variations of atmospheric CO₂ and CH₄ mixing ratio due to
19 emissions in the Los Angeles megacity.

20 On the other hand, the west Pasadena and Santa Anita Park reflection points exhibited strong
21 diurnal signals in XCO₂ and XCH₄, with a minimum typically in the early morning of around
22 405-410 ppm for XCO₂ and 1800-1900 ppb for XCH₄ and a maximum of up to 420 ppm for
23 XCO₂ and 1950 ppb for XCH₄ at noon or in the early afternoon. Variability in CO₂ and CH₄
24 emissions and atmospheric transport resulted in daily ranges of variation of 10-30 ppm XCO₂
25 and 100-200 ppb XCH₄ during the period of May 5-11, 2012. With a typical boundary layer
26 height, the west Pasadena and the Santa Anita Park measurements sample horizontally over a
27 few kilometers in the PBL and are therefore sensitive to emission signatures. The buildup of
28 XCO₂ and XCH₄ in the morning and the falloff in the afternoon are due to a combination of
29 accumulation of emissions and dilution/advection processes in basin. Similar diurnal patterns of
30 XCO₂ and XCH₄ (that is, peak at noon or early afternoon) have been observed in Pasadena by a

1 TCCON station (Wunch et al., 2009). However, the column enhancements observed by TCCON
2 are typically less than 2–3 ppm in XCO₂ and 20–40 ppb in XCH₄. These enhancements are
3 significantly smaller than those derived from the CLARS-FTS measurements which have a
4 longer optical path within the PBL compared with TCCON at the same SZA.

5
6 Variations in PBL height do not affect the diurnal profile of XCO₂ and XCH₄ as they would in in
7 situ measurements, in which diurnal variation is often characterized by GHG concentration peaks
8 in the morning and evening when the PBL is shallow and a minimum in midday when the PBL
9 has grown (Newman et al., 2013). This is because XCO₂ and XCH₄ are derived from the slant
10 column abundance along the CLARS-FTS optical paths. This is valid as long as the PBL height
11 is below Mount Wilson. Since the PBL typically locates below Mount Wilson (Newman et al.,
12 2013), this is a major advantage of column measurements over in situ measurements.

13 **3.2 Slopes of derived CH₄:CO₂ correlations**

14 Several studies have reported strong correlations between CH₄ and CO₂ measured in the PBL in
15 source regions (Peischl et al., 2013; Wennberg et al., 2012; Wunch et al., 2009; S. Newman,
16 personal communication, 2014). Slopes of CH₄:CO₂ correlation plots have been identified with
17 local emission ratios for the two gases. Since the uncertainty in CH₄ emissions is considerably
18 larger than that in CO₂ emissions, we may use the correlation slope to reduce the CH₄ emission
19 uncertainties. [A few assumptions are used when quantifying CH₄ emission based on CH₄:CO₂
20 correlation. These assumptions will be discussed in Section 4.1 of the paper.](#) In this study, we
21 determined the spatial variation of CH₄:CO₂ ratios originating from CLARS-FTS measurements
22 between September 2011 and October 2013. It is first necessary to remove the background
23 variations in CO₂ and CH₄ in order to calculate the concentration anomalies resulting from
24 emissions in the PBL. Different approaches to deriving the background concentrations were
25 considered including using the early morning, daily minimum and daily average XGHG for each
26 reflection point. However, because of variations in the yield of LABS data passing through the
27 data filters, biases may be introduced into the background estimation by these methods. As a
28 result, we determined that the SVO observations, which have a very small diurnal variation, are
29 the most appropriate background reference values for the CLARS LABS measurements. The

1 excess XCO₂ and XCH₄ above background in the Los Angeles megacity are simply calculated by
2 subtracting the SVO observations from the LABS observations (Eq. 2).

$$3 \quad \text{XGHG}_{(\text{XS})} = \text{XGHG}_{\text{LABS}} - \text{XGHG}_{\text{SVO}} \quad (2)$$

4 We used orthogonal distance regression (ODR) analysis, [which considers uncertainties in both](#)
5 [XCH_{4\(XS\)} and XCO_{2\(XS\)}](#), to quantify the emissions of CH₄ relative CO₂ in the Los Angeles
6 megacity. Using this approach, we find values of 7.3±0.1 ppb CH₄ (ppm CO₂)⁻¹ for the west
7 Pasadena reflection point and 6.1±0.1 ppb CH₄ (ppm CO₂)⁻¹ for the Santa Anita Park reflection
8 point. Fig. 4 illustrates the tight correlations found between XCH_{4(XS)} and XCO_{2(XS)} for each
9 reflection point. The tight correlations imply that there is not substantial difference in the
10 emission ratio of the two GHGs during the measurement period from 2011 to 2013. XCH_{4(XS)} and
11 XCO_{2(XS)} should be poorly correlated with each other if their emission ratio varies largely over
12 time, assuming the correlation is mainly driven by emissions.

13 [Table 3 lists the correlation slopes and their uncertainties for the 28 basin reflection points.](#)
14 Figure 5 maps the observed XCH_{4(XS)}/XCO_{2(XS)} correlation slopes (in units of ppb CH₄ (ppm
15 CO₂)⁻¹) across the Los Angeles megacity using natural neighbor interpolation (Sibson, 1981).
16 The mean [± one standard deviation](#) for all 28 reflection points was 6.4±0.5 ppb CH₄ (ppm CO₂)⁻¹
17 with individual values ranging from 5.4 to 7.3 ppb CH₄ (ppm CO₂)⁻¹. Elevated XCH_{4(XS)}/XCO_{2(XS)}
18 ratios were observed in west Pasadena and in the eastern side of the Los Angeles megacity.

19 Spatial gradients among reflection points became weaker as distance from Mount Wilson
20 increased. Stronger spatial gradients were observed among the closer reflection points in the
21 basin, that is, west Pasadena, Santa Anita Park and East Los Angeles, while weaker spatial
22 gradients were observed among the more distant reflection points, such as Long Beach, Marina
23 Del Rey and North Orange County. Measurements were averaged over a much longer slant path
24 for the more distant reflection points, compared to the nearby reflection points, making the
25 measurements for the more distant reflection points less sensitive to local/point sources.
26 Bootstrap analysis (Efron and Tibshirani, 1993) was performed to make sure that the spatial
27 variations of the correlation slopes were not a result of sampling bias among the 28 reflection
28 points. The uncertainties in the correlation slopes became larger with increasing distance from
29 Mount Wilson due to the decreased data quality, as the measurement path in the Los Angeles

1 megacity became longer. (More data were filtered out for targets further from the instrument,
2 mostly because of aerosol loading.)

3 The CLARS-FTS observations in west Pasadena are in good agreement with TCCON
4 measurements at the Jet Propulsion Laboratory, which showed a ratio of 7.8 ± 0.8 ppb CH_4
5 $(\text{ppm CO}_2)^{-1}$ (Wunch et al., 2009). Subtle differences between the TCCON and the CLARS-FTS
6 are due to the relative change in the ratio over time, difference measurement geometry, and/or
7 the different approach in determining the excess ratio. A number of in situ ground and aircraft
8 measurements of CO_2 and CH_4 have been performed recently in the goal of quantifying GHG
9 emissions in the megacity. A list of $\text{CH}_4:\text{CO}_2$ ratios reported by these observations is shown in
10 Table 4. These observations reported ratios ranging from 6.10 to 6.74 ppb CH_4 $(\text{ppm CO}_2)^{-1}$
11 (Wennberg et al., 2012; Peischl et al., 2013; S. Newman, personal communication, 2014; Y.-K.
12 Hsu, personal communication, 2014). At California Institute of Technology (Caltech) in
13 Pasadena and at the CLARS facility on Mount Wilson, in situ CH_4 and CO_2 mixing ratios were
14 measured by two Picarro G1301 $\text{CO}_2\text{-CH}_4$ analyzers (Newman et al., 2013). Secondary
15 standards, calibrated against primary NOAA standards, were run every 11 hours. Because of the
16 complex boundary layer dynamics near mountains, measurements on Mount Wilson is
17 influenced by upslope flow of air mass from the basin during the day while expose to the clean
18 background air from the free tropospheric at night (Hsu et al., 2009). Using the mean of hourly
19 averages from 22:00 – 03:00 PST on Mount Wilson as the background reference, CH_4 and CO_2
20 excess mixing ratios were calculated by subtracting the background reference from the daytime
21 hourly averaged measurements at Mount Wilson and at Caltech. The ratios were the correlation
22 slopes between the two. Because of the different measurement techniques, measurement periods
23 and locations, $\text{CH}_4:\text{CO}_2$ ratios reported by these studies are not directly comparable to column
24 measurements. However, the CLARS-FTS observations of $\text{CH}_4:\text{CO}_2$ ratios show consistency
25 with these measurements.

26

27 **4 Discussion**

28 **4.1 Analysis assumptions**

1 A number of assumptions are involved in deriving the $\text{CH}_4:\text{CO}_2$ emission ratios. These are
2 described in this subsection.

- 3 • $\text{XCH}_{4(\text{XS})}$ and $\text{XCO}_{2(\text{XS})}$ are correlated even though the two GHGs are not emitted from the
4 same sources. CH_4 and CO_2 have chemical lifetimes that are much longer than the
5 timescales for mesoscale transport and therefore behave like inert tracers in the boundary
6 layer. Even if emitted from different sources, atmospheric processes in the boundary
7 layer will result in mixing on relatively short timescales (typical mixing timescale in the
8 PBL is on the order of 10-20 min, Stull, 1988). CLARS-FTS samples air masses that
9 have undergone this short timescale mixing. The high degree of correlation observed
10 between $\text{XCH}_{4(\text{XS})}$ and $\text{XCO}_{2(\text{XS})}$ for all 28 reflection points supports this mixing
11 assumption over the entire area of the LA basin.
- 12 • The slope of the $\text{XCH}_{4(\text{XS})}:\text{XCO}_{2(\text{XS})}$ correlation observed at each LABS measurement
13 point is sensitive to both the relative emissions over a horizontal path weighted toward
14 the reflection point, and the composition of the air mass advected into the atmospheric
15 path. The long optical path in the boundary layer and the effect of advection smear out
16 the effects of local emission ratio variations. This smearing is different for each reflection
17 point. Future work will deconvolve these effects using an atmospheric transport model
18 which will include advection, boundary layer mixing, surface emissions and ray-tracing
19 of the optical path sampled by CLARS-FTS on a 1-2 km grid.
- 20 • The effect of aerosol scattering on the $\text{XCH}_{4(\text{XS})}:\text{XCO}_{2(\text{XS})}$ slopes is assumed to be
21 negligible. Using a two-stream numerical radiative transfer model constrained by
22 AERONET aerosol optical depths in the near-infrared, Zhang et al. (2014) showed that
23 the bias in the retrieved XCO_2 from CLARS-FTS LABS measurements does not exceed
24 1%, using data that have passed the filter criteria described above. This bias is caused by
25 the wavelength dependence of aerosol scattering and absorption between the CO_2
26 absorption band at 1.61 μm , and the O_2 absorption band at 1.27 μm . Further analysis
27 based on Zhang et al. (2014) indicates that the aerosol-induced bias on XCO_2 and XCH_4
28 is nearly identical and cancel out in the ratio since the CO_2 and CH_4 observations used in
29 this analysis are retrieved at nearly identical wavelengths (1.61 μm vs. 1.66 μm). The
30 uncertainty of $\text{XCH}_4:\text{XCO}_2$ ratio due to aerosol is negligible (<0.5%). Uncertainties due

1 to aerosol scattering on the CLARS-FTS XCO_2 and XCH_4 observations will be reduced
2 significantly in the next version of the CLARS-FTS retrieval algorithm which will
3 consider aerosol scattering explicitly in the forward model (Zhang et al., 2014).

- 4 • The number of discrete reflection points (28 plus the direct solar path) is sufficient to
5 characterize the average emission ratio over the Los Angeles megacity. The CLARS-FTS
6 LABS mode spans slant distances in the range 4-40 km in the Los Angeles PBL, and
7 therefore should have sufficient spatial coverage of the megacity. In the future, sensitivity
8 studies will be performed to optimize the spatial distribution of the reflection points with
9 respect to coverage of emission sources, aerosol bias, albedo variability, locations of
10 other stations in the monitoring network, and other parameters.
- 11 • Seasonal bias in the $XCH_{4(XS)}:XCO_{2(XS)}$ correlation slope is small. Certain times of the
12 year are more likely to be influenced by cloud and aerosol events in Los Angeles and
13 have correspondingly fewer measurements that pass the data quality filters. The fraction
14 of data passing through the data filter varies by a factor of two in different seasons. In our
15 analysis the effect of seasonal bias is small. This seems to be a reasonable assumption
16 since tight correlation was observed between $XCH_{4(XS)}$ and $XCO_{2(XS)}$ throughout the year,
17 the contribution of seasonal sampling bias, if any, has a negligible effect on the random
18 error of the annual average $XCH_{4(XS)}:XCO_{2(XS)}$ correlation slope.
- 19 • Spatial variation in the atmospheric column of CO_2 and CH_4 above Mount Wilson is
20 minimal and does not affect the $XCH_4:XCO_2$ excess ratio. Spatial variation in CO_2 and
21 CH_4 mixing ratio above Mount Wilson in the basin is possible due to entrainment of
22 boundary layer air mass into the free troposphere and long-range transport. It can be
23 shown that spatial variability in the column above Mount Wilson due to entrainment of
24 boundary layer height or long-range transport adds less than 1% uncertainty to
25 $XCH_4:XCO_2$ excess ratio.

26 4.2 Top-down CH_4 emissions from CLARS-FTS observations

27 With the assumptions described in the previous subsection, we estimate the top-down annual
28 CH_4 emission for the Los Angeles megacity based on the CLARS-FTS observations. In this
29 analysis, we define the Los Angeles megacity as the spatial domain of the South Coast Los
30 Angeles basin. The CARB reported an annual statewide CO_2 emission of 387 Tg CO_2 /year for

1 2011 (http://www.arb.ca.gov/app/ghg/2000_2011/ghg_sector.php). Since the majority of CO₂
 2 emissions are from fossil fuel combustion, we assumed that the CO₂ emissions are spatially
 3 distributed by population in the state. We apportioned the statewide emissions by population in
 4 the Los Angeles megacity, which is 43% of statewide population, to estimate the bottom-up
 5 emission for the Los Angeles megacity (<http://www.census.gov/>). The bottom-up CO₂ emission
 6 inventory for the Los Angeles megacity was thus 166±23 Tg CO₂ year⁻¹ in 2011, assuming 10%
 7 uncertainties in both the CARB statewide CO₂ emission and the spatial distribution of emissions
 8 by population. For the bottom-up CH₄ emission in the Los Angeles megacity, we used the same
 9 method as in Wunch et al. (2009) and Peischl et al. (2013). [Agriculture and forestry contributes](#)
 10 [62% of total CH₄ emission in the state \(California Air Resources Board, 2011\)](#) but the [Los](#)
 11 [Angeles basin contains less than 2% of farmlands in California \(United States Department of](#)
 12 [Agriculture, 2012\)](#). Therefore we estimated the bottom-up CH₄ emissions in the basin by
 13 [subtracting agriculture and forestry sector from the total statewide emission then apportioned by](#)
 14 [population](#). This gave a bottom-up CH₄ emission inventory of 0.28 Tg CH₄ year⁻¹ in the Los
 15 Angeles megacity in 2011. Using the bottom-up emission inventory of CO₂ for the Los Angeles
 16 megacity (166±23 Tg CO₂ year⁻¹) and the CH₄:CO₂ ratio observed by the CLARS-FTS (6.4±0.5
 17 [ppb CH₄ \(ppmCO₂\)⁻¹](#)), we derived the CH₄ emission inventory using Eq. 3, where E_{CH₄|top-down}
 18 is the top-down CH₄ emissions inferred by the CLARS-FTS observations, E_{CO₂|bottom-up} is the
 19 bottom-up CO₂ emissions, $\frac{X_{CH_4}}{X_{CO_2}}|_{slope}$ is the X_{CH₄(XS)}/X_{CO₂(XS)} ratio observed by the FTS and
 20 $\frac{MW_{CO_2}}{MW_{CH_4}}$ is the ratio of molecular weight of CO₂ and CH₄ (that is, 16 g CH₄/ 44 g CO₂).

$$21 \quad E_{CH_4|top-down} = E_{CO_2|bottom-up} \times \frac{X_{CH_4}}{X_{CO_2}}|_{slope} \times \frac{MW_{CH_4}}{MW_{CO_2}} \quad (3)$$

22 The derived CH₄ emission inventory was 0.39±0.06 Tg CH₄ year⁻¹ in the Los Angeles megacity
 23 assuming a 10% uncertainty in the CARB bottom-up CO₂ emission. The derived CH₄ emission
 24 inventory was 18–61 % larger than the bottom-up emission inventory in 2011. This is in good
 25 agreement with [the top-down CH₄ emissions from recent studies \(Wunch et al., 2009; Hsu et al.,](#)
 26 [2010; Wennberg et al., 2012; Peischl et al., 2013; Jeong et al. 2013\)](#) and [the CH₄ emissions](#)
 27 [derived from the observations at Caltech and on Mount Wilson \(using the same bottom-up CO₂](#)
 28 [emissions for the Los Angeles basin\)](#).

1 Because of the spatial and temporal variations of CH₄:CO₂ ratio in the Los Angeles megacity, the
2 derived CH₄ emission based on local observations can be biased. For instance, if we were to
3 evaluate the bottom-up CH₄ emission inventory by our observations in west Pasadena only, the
4 derived CH₄ emission inventory for the Los Angeles megacity would be overestimated by 14%,
5 since the west Pasadena target observed a CH₄:CO₂ slope that is 14% larger than the average
6 slope of the 28 reflection points. Therefore, to quantify and to reduce uncertainties in carbon
7 emissions from the Los Angeles megacity or any other urban areas which are highly
8 heterogeneous, it is important to have measurements which provide both spatial and temporal
9 coverage. It is challenging to quantify individual point sources of CH₄. Further investigations
10 need to be performed to link the CLARS-FTS observations to emissions from landfills, oil
11 extraction and natural gas pipeline leakage.

12 **4.3 Relevance to future satellite GHG observations**

13 This study has shown that spatially resolved CH₄:CO₂ emission ratio measurements can be made
14 over a megacity domain (hundreds of km²) using a remote sensing method that simulates the
15 observations from an imaging spectrometer such as GEO-FTS from geostationary orbit. From
16 GEO, the field of regard is approximately one-third of the Earth below 60 deg latitude. Operating
17 as a hosted payload from a commercial communications satellite, measurements of XCO₂, XCH₄,
18 XCO and solar-induced chlorophyll fluorescence (SIF) will be made every 1-2 h during daylight
19 with a pixel footprint of 2-3 km at the sub-satellite point with retrieval precisions comparable to
20 those obtained from CLARS-FTS (Fu et al., 2014). In the near future, a two-dimensional
21 imaging FTS similar to GEO-FTS will be deployed at CLARS to increase the spatial density of
22 the retrievals.

23

24 **5 Conclusions**

25 This study is the first to map GHGs in the Los Angeles megacity using ground-based remote
26 sensing technique. It combines the unique vista from Mount Wilson and high-sensitivity
27 measurements made by the CLARS-FTS to simulate satellite observations. Persistent space and
28 time resolved observations of GHG in the Los Angeles megacity over a two-year period in 2011-

1 2013 and a tracer-to-tracer correlation analysis are used to reveal an interesting spatial pattern of
2 CH₄:CO₂ ratio in the megacity. The slope of the correlations between XCH_{4(XS)} and XCO_{2(XS)}
3 showed significant spatial variations ranging from 5.4 to 7.3 ppb CH₄ (ppm CO₂)⁻¹, with an
4 average of 6.4±0.5 ppb CH₄ (ppm CO₂)⁻¹, indicating that there is spatial heterogeneity in the
5 megacity. Using the CARB bottom-up emission inventory of CO₂, we derived the CH₄ emission
6 inventory of the Los Angeles megacity in 2011-2013 to be 0.39±0.06 Tg CH₄ year⁻¹, which was
7 18–61% above the bottom-up CH₄ emission inventory. Good agreements among previous
8 aircraft observations and local observations indicated the CLARS-FTS to be a robust
9 measurement technique that can quantify and track GHG emissions in the Los Angeles megacity
10 in an efficient way. The CLARS-FTS also demonstrates the potential success for future satellite
11 mission to quantify carbon emissions from megacities from space. The heterogeneity
12 characteristics in the megacity can lead to a 14% uncertainty in the derived top-down CH₄
13 emissions if only observations in west Pasadena are used. However, due to the complexity of the
14 measurement geometry of the CLARS-FTS observations, it is challenging to pinpoint local
15 sources or to derive a map of local CH₄:CO₂ emission ratios at this point. Additional future work
16 needs to be done. The CLARS-FTS observations, which span the Los Angeles megacity
17 continuously, fill the gap between the local measurements that provide long-term observations
18 but are too sensitive to local emissions, and aircraft data that provides intense spatial and
19 temporal observations yet are too expensive to carry out continuously throughout the year.
20 However, it is necessary to combine the CLARS-FTS observations with in situ ground and
21 aircraft data for a long-term GHG monitoring effort in the megacity.

22 **Acknowledgements**

23 The authors thank our colleagues and D. Wunch (California Institute of Technology), J. Stutz
24 (University of California, Los Angeles) and G. Keppel-Aleks (University of Michigan) for
25 helpful comments. Support from NASA Postdoctoral Program, California Air Resources Board,
26 NOAA Climate Program, NIST GHG and Climate Science Program and JPL Earth Science and
27 Technology Directorate is gratefully acknowledged. YLY was supported in part by NASA grant
28 NNX13AK34G to the California Institute of Technology and the KISS program of Caltech.

1 References

- 2 Aben, I., Hasekamp, O., and Hartmann, W.: Uncertainties in the space-based measurements of
3 CO₂ columns due to scattering in the Earth's atmosphere, *J. Quant. Spectrosc. Ra.*, 104, 450–
4 459, 2007.
5
- 6 Crisp, D., Fisher, B. M., O'Dell, C., Frankenberg, C., Basilio, R., Bösch, H., Brown, L. R.,
7 Castano, R., Connor, B., Deutscher, N. M., Eldering, A., Griffith, D., Gunson, M., Kuze, A.,
8 Mandrake, L., McDuffie, J., Messerschmidt, J., Miller, C. E., Morino, I., Natraj, V., Notholt,
9 J., O'Brien, D. M., Oyafuso, F., Polonsky, I., Robinson, J., Salawitch, R., Sherlock, V.,
10 Smyth, M., Suto, H., Taylor, T. E., Thompson, D. R., Wennberg, P. O., Wunch, D., and
11 Yung, Y. L.: The ACOS CO₂ retrieval algorithm – Part II: Global XCO₂ data
12 characterization, *Atmos. Meas. Tech.*, 5, 687–707, doi:10.5194/amt-5-687-2012, 2012.
13
- 14 [de la Rue du Can, S., Wenzel, T., and Price, L.: Improving the Carbon Dioxide Emission](#)
15 [Estimates from the Combustion of Fossil Fuels in California, Report prepared for the](#)
16 [California Air Resources Board and the California Environmental Protection Agency, 2008.](#)
17
- 18 Efron, B. and Tibshirani, R.: *An Introduction to the Bootstrap*, Vol. 57, CRC press, Boca Raton,
19 Florida, USA, 1993.
20
- 21 Fu, D., Pongetti, T. J., Blavier, J.-F. L., Crawford, T. J., Manatt, K. S., Toon, G. C., Wong, K.
22 W., and Sander, S. P.: Near-infrared remote sensing of Los Angeles trace gas distributions
23 from a mountaintop site, *Atmos. Meas. Tech.*, 7, 713–729, doi:10.5194/amt-7-713-2014,
24 2014.
25
- 26 Hsu, Y.-K., VanCuren, T., Park, S., Jakober, C., Herner, J., FitzGibbon, M., Blake, D. R., and
27 Parrish, D. D.: Methane emissions inventory verification in southern California, *Atmos.*
28 *Environ.*, 44, 1–7, 2010.
29
- 30 Jeong, S., Hsu, Y.-K., Andrews, A. E., Bianco, L., Vaca, P., Wilczak, J. M., and Fischer, M. L.:
31 A multitower measurement network estimate of California's methane emissions, *J. Geophys.*
32 *Res.-Atmos.*, 118, 11339–11351, doi:10.1002/jgrd.50854, 2013.
33
- 34 Key, R., Sander, S., Eldering, A., Blavier, J.-F., Bekker, D., Manatt, K., Rider, D., and Wu, Y.-H.:
35 The geostationary fourier transform spectrometer, *Proc. SPIE*, 8515, doi:10.1117/12.930257,
36 2012.
37
- 38 Kort, E. A., Angevine, W. M., Duren, R., and Miller, C. E.: Surface observations for monitoring
39 urban fossil fuel CO₂ emissions: Minimum site location requirements for the Los Angeles
40 megacity, *J. Geophys. Res.-Atmos.*, 118, 1577–1584, doi:10.1002/jgrd.50135, 2013.
41
- 42 Mandrake, L., Frankenberg, C., O'Dell, C. W., Osterman, G., Wennberg, P., and Wunch,
43 D.: Semi-autonomous sounding selection for OCO-2, *Atmos. Meas. Tech.*, 6, 2851–2864,
44 doi:10.5194/amt-6-2851-2013, 2013.
45

- 1 Newman, S., Jeong, S., Fischer, M. L., Xu, X., Haman, C. L., Lefer, B., Alvarez, S.,
2 Rappenglueck, B., Kort, E. A., Andrews, A. E., Peischl, J., Gurney, K. R., Miller, C. E., and
3 Yung, Y. L.: Diurnal tracking of anthropogenic CO₂ emissions in the Los Angeles basin
4 megacity during spring 2010, *Atmos. Chem. Phys.*, 13, 4359–4372, doi:10.5194/acp-13-
5 4359-2013, 2013.
- 6
- 7 O'Dell, C. W., Connor, B., Bösch, H., O'Brien, D., Frankenberg, C., Castano, R., Christi, M.,
8 Eldering, D., Fisher, B., Gunson, M., McDuffie, J., Miller, C. E., Natraj, V., Oyafuso, F.,
9 Polonsky, I., Smyth, M., Taylor, T., Toon, G. C., Wennberg, P. O., and Wunch, D.: The
10 ACOS CO₂ retrieval algorithm – Part 1: Description and validation against synthetic
11 observations, *Atmos. Meas. Tech.*, 5, 99–121, doi:10.5194/amt-5-99-2012, 2012.
- 12
- 13 Peischl, J., Ryerson, T. B., Brioude, J., Aikin, K. C., Andrews, A. E., Atlas, E., Blake, D., Daube,
14 B. C., de Gouw, J. A., Dlugokencky, E., Frost, G. J., Gentner, D. R., Gilman, J. B.,
15 Goldstein, A. H., Harley, R. A., Holloway, J. S., Kofler, J., Kuster, W. C., Lang, P. M.,
16 Novelli, P. C., Santoni, G. W., Trainer, M., Wofsy, S. C., and Parrish, D. D.: Quantifying
17 sources of methane using light alkanes in the Los Angeles basin, California, *J. Geophys.*
18 *Res.-Atmos.*, 118, 4974–4990, doi:10.1002/jgrd.50413, 2013.
- 19
- 20 Sibson, R.: A brief description of natural neighbor interpolation, in: *Interpreting Multivariate*
21 *Data*, edited by: Barnett, V., Wiley, Chichester, 21–36, 1981.
- 22
- 23 Spurr, R. J: VLIDORT: A linearized pseudo-spherical vector discrete ordinate radiative transfer
24 code for forward model and retrieval studies in multilayer multiple scattering media, *J.*
25 *Quant. Spectrosc. RA.*, 102, 2, 316–342, 2006.
- 26
- 27 Stull, R: *An Introduction to Boundary Layer Meteorology*, Springer, the Netherlands, 1988.
- 28
- 29 Washenfelder, R. A. and Wennberg, P. O.: Tropospheric methane retrieved from ground-based
30 near-IR solar absorption spectra, *Geophys. Res. Lett.*, 30, 23, 2226,
31 doi:10.1029/2003GL017969, 2003.
- 32
- 33 Washenfelder, R. A., Toon, G. C., Blavier, J.-F., Yang, Z., Allen, N. T., Wennberg, P. O., Vay,
34 S. A., Matross, D. M., and Daube, B. C.: Carbon dioxide column abundances at the
35 Wisconsin Tall Tower site, *J. Geophys. Res.*, 111, D22305, doi:10.1029/2006JD007154,
36 2006.
- 37
- 38 Wennberg, P. O., Mui, W., Wunch, D., Kort, E. A., Blake, D. R. Atlas, E. L., Santoni, G. W.,
39 Wofsy, S. C., Diskin, G. S., Joeng, S., and Fischer, M. L.: On the sources of methane to the
40 Los Angeles atmosphere, *Environ. Sci. Technol.*, 46, 9282–9289, doi:10.1021/es301138y,
41 2012.
- 42
- 43 Wunch, D., Wennberg, P. O., Toon, G. C., Keppel-Aleks, G., and Yavin, Y. G.: Emissions of
44 greenhouse gases from a North American megacity, *Geophys. Res. Lett.*, 36, L15810,
45 doi:10.1029/2009GL039825, 2009.
- 46

- 1 Wunch, D., Toon, G. C., Blavier, J. L., Washenfelder, R. A., Notholt, J., Connor, B. J., Griffith,
2 D. W., Sherlock, V., and Wennberg, P. O.: The total carbon column observing network,
3 *Philos. T. Roy. Soc. A*, 369, 2087–2112, 2011.
4
- 5 Yoshida, Y., Ota, Y., Eguchi, N., Kikuchi, N., Nobuta, K., Tran, H., Morino, I., and Yokota, T.:
6 Retrieval algorithm for CO₂ and CH₄ column abundances from short-wavelength infrared
7 spectral observations by the Greenhouse Gases Observing Satellite, *Atmos. Meas. Tech.*, 4,
8 4, 717–734, 2011.
9
- 10 Zhang, Q., Natraj, V., Li, K., Shia, R., Fu, D., Pongetti, T., Sander, S. P., and Yung, Y. L.:
11 Influence of aerosol scattering on the retrieval of CO₂ mixing ratios: a case study using
12 measurements from the California Laboratory for Atmospheric Remote Sensing (CLARS),
13 *Geophys. Res. Lett.*, in preparation, 2014.
14
- 15 United States Department of Agriculture, The Census of Agriculture: 2012 Census Publications,
16 technical report, U.S. Dep. Agric., Washington, D. C., last access: August 2014.
- 17 California Air Resources Board: Greenhouse gas emission inventory – Query tool for years 2000
18 to 2011, 6th Edn., http://www.arb.ca.gov/app/ghg/2000_2011/ghg_sector.php, last access:
19 January 2014.

1 Table 1. List of the 29 reflection points on Mount Wilson and in the Los Angeles megacity.

	Target	Latitude	Longitude	Slant distance from FTS (km)	*Slant path in PBL (km)	Footprint (km²)
1	Spectralon®, Mount Wilson	34.22	-118.06	0.01	0	0
2	Santa Anita Park	34.14	-118.04	9.2	4.2	0.04
3	west Pasadena	34.17	-118.17	11.5	5.9	0.09
4	Santa Fe Dam	34.11	-117.97	14.9	6.8	0.17
5	East Los Angeles	34.05	-118.12	20.2	9.2	0.41
6	Fwy 210	34.12	-117.87	20.9	10.1	0.49
7	Downtown (near)	34.10	-118.23	21.1	9.6	0.47
8	Glendale	34.15	-118.27	21.4	10.0	0.50
9	Fwys 60 and 605	34.03	-118.03	21.7	9.5	0.49
10	Universal City	34.14	-118.35	28.8	13.4	1.23
11	Fwy 60, City of Industry	34.00	-117.88	29.6	13.7	1.33
12	Downtown (far)	34.05	-118.31	29.7	12.9	1.25
13	Downey	33.93	-118.16	33.9	14.5	1.84
14	La Mirada	33.91	-118.01	35.2	15.3	2.09
15	Pomona	34.04	-117.73	36.7	18.1	2.70
16	Santa Monica Mountains	34.09	-118.47	40.9	20.2	3.74

17	Marina Del Rey	33.99	-118.40	41.0	17.3	3.22
18	Rancho Cucamonga	34.08	-117.59	46.1	24.0	5.66
19	Long Beach	33.82	-118.20	46.5	19.6	4.70
20	North Orange County	33.86	-117.78	47.8	21.3	5.38
21	Angels Stadium	33.80	-117.88	49.8	21.5	5.89
22	Norco	33.96	-117.57	53.5	25.3	8.01
23	Palos Verdes	33.81	-118.37	54.2	23.7	7.70
24	Huntington Beach	33.72	-117.98	56.2	23.8	8.32
25	Corona	33.87	-117.60	56.0	28.8	10.71
26	Orange Country Airport	33.68	-117.86	63.3	26.7	11.86
27	Fontana	34.07	-117.39	64.3	33.8	15.46
28	Riverside	33.95	-117.39	68.5	34.1	17.75
29	Lake Mathews	33.88	-117.42	70.7	39.1	21.62

1 *Slant paths in PBL are estimated assuming a uniform PBL height of 700 m, which was the
2 average PBL height observed during CalNex 2010.

3

1 Table 2. Data filter criteria.

Filter	Criteria
High clouds	$SVO O_2_{SCD_retrieved} : O_2_{SCD_geometric} > 1.1$ or < 1
Low clouds and/or aerosol	$LABS O_2_{SCD_retrieved} : O_2_{SCD_geometric} > 1.1$ or < 0.9
Large SZA	$SZA > 70$ degree
Low SNR	$SNR < 100$
Poor spectral fitting	Fitting residual RMS > 1 standard deviation above average

2

1 Table 3. List of correlation slopes of $XCH_{4(xS)}:XCO_{2(xS)}$ and their uncertainties (one standard
 2 deviation) observed by the CLARS-FTS between the period of September 2011 and October
 3 2013.

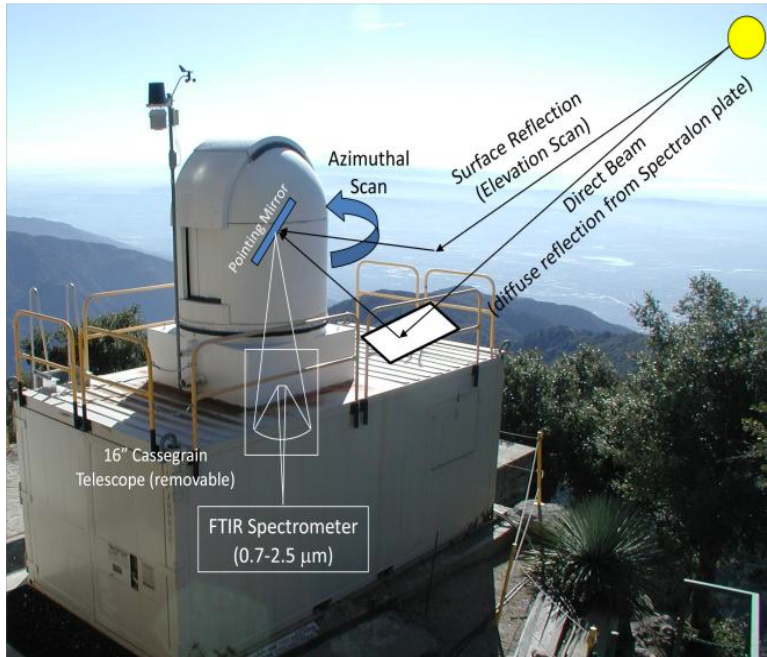
Target	$XCH_{4(xS)}/$ $XCO_{2(xS)}$ (ppb/ppm)	Uncertainties (ppb/ppm)
Santa Anita Park	6.09	0.05
west Pasadena	7.28	0.09
Santa Fe Dam	5.85	0.12
East Los Angeles	5.99	0.15
Fwy 210	6.26	0.20
Downtown (near)	6.42	0.21
Glendale	6.04	0.20
Fwys 60 and 605	7.34	0.31
Universal City	6.47	0.28
Fwy 60, City of Industry	7.25	0.41
Downtown (far)	6.33	0.23
Downey	6.24	0.29
La Mirada	7.13	0.35
Pomona	6.52	0.25
Santa Monica Mountains	6.55	0.33
Marina Del Rey	6.75	0.27
Rancho Cucamonga	5.35	0.15
Long Beach	6.18	0.28

North OC	6.41	0.35
Angels Stadium	6.65	0.39
Norco	6.87	0.31
Palos Verdes	6.59	0.34
Huntington Beach	6.10	0.24
Corona	6.40	0.30
Orange Country Airport	5.99	0.29
Fontana	6.18	0.23
Riverside	6.40	0.32
Lake Mathews	5.99	0.23

-
- 1 [*The uncertainties include only fitting uncertainties. Systematic uncertainties of ~4% were](#)
 - 2 [not taken account here \(Fu et al., 2014\).](#)

1 Table 4. Comparisons of CH₄:CO₂ ratios and derived top-down CH₄ emissions among various
 2 measurements in the Los Angeles megacity. [Wunch et al. \(2009\)](#) reported two top-down CH₄
 3 estimates: 0.40±0.10 Tg CH₄ year⁻¹ derived from CH₄:CO₂ ratio and 0.60±0.10 Tg CH₄ year⁻¹
 4 derived from CH₄:CO ratio. Please note that it is difficult to compare the uncertainties due to the
 5 different measurement techniques.

Measurement (Location, period)	CH₄:CO₂ ratio (ppb:ppm)	Derived top-down CH₄ emission (Tg CH₄/ year)	Measurement type	References
TCCON (Pasadena, 8/2007 – 6/2008)	7.80±0.80	0.40 ± 0.10 0.60 ± 0.10	Column (FTS)	Wunch et al. 2009
ARCTAS (LA , 6/2008)	6.74±0.58	0.47 ± 0.10	Aircraft in situ (Picarro)	Wennberg et al. 2012
CalNex (LA , 5/2010 – 6/2010)	6.70±0.01 6.55±0.29	0.41 ± 0.04 0.44 ± 0.10	Aircraft in situ (Picarro)	Peischl et al. 2013 Wennberg et al. 2012
Caltech (Pasadena, 2/2012-8/2012)	6.30±0.01	0.38 ± 0.05	Surface in situ	This study
Mount Wilson (Pasadena, 9/2011-6/2013)	6.10±0.10	0.37 ± 0.05	Surface in situ (Picarro)	This study
CLARS-FTS, Mount Wilson (LA , 9/2011 – 10/2013)	6.40±0.50	0.39 ± 0.06	Column (FTS)	This study



1



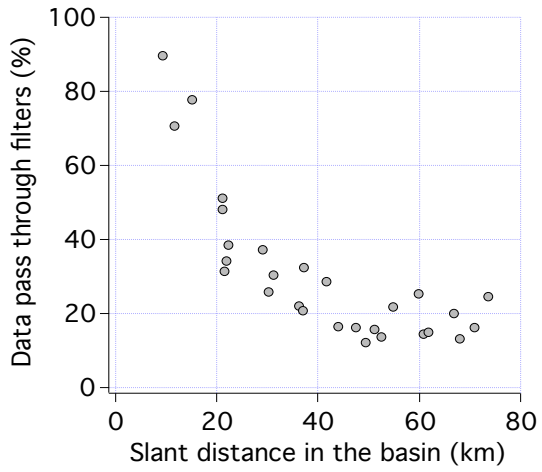
2

3 Figure 1. The CLARS-FTS on Mount Wilson (top) and its 29 reflection points on Mount Wilson
 4 and in the Los Angeles megacity (bottom). Reflection points are labeled in the order of
 5 increasing distance from the FTS. Information of the reflection points is given in Table 1. A
 6 small fraction of the central Los Angeles megacity area cannot be viewed from Mount Wilson
 7 due to a nearby mountain peak.

8

1

2

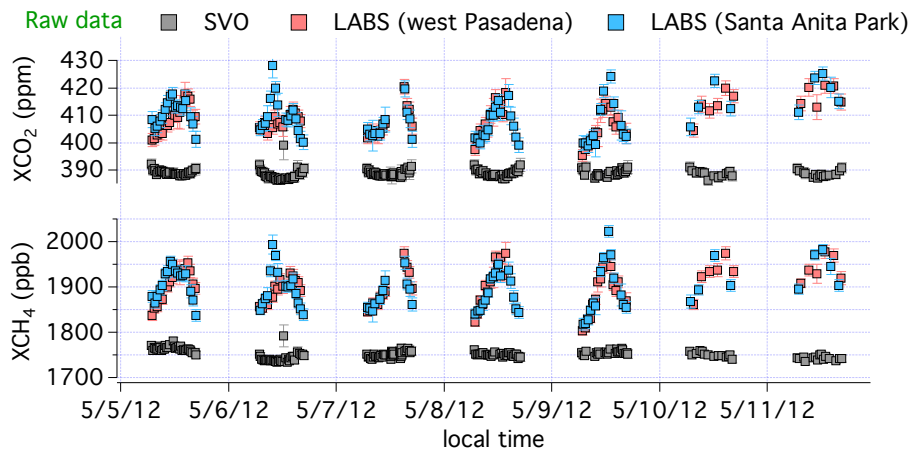


3

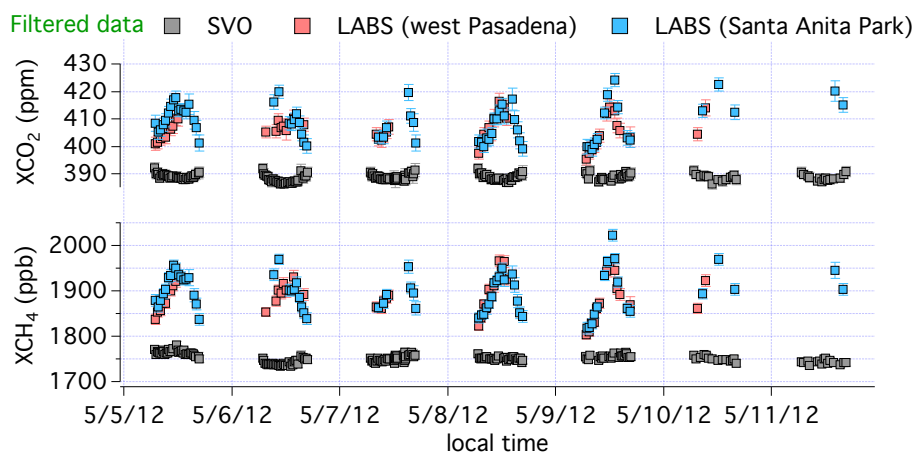
4 Figure 2. Percent of data points that pass through our data filters as a function of slant distance in
5 the Los Angeles megacity.

6

7



1

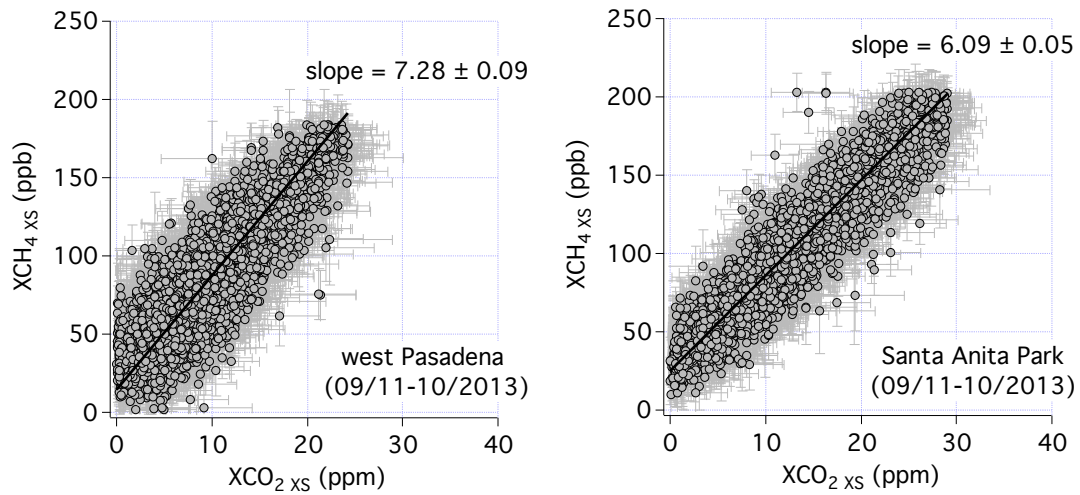


2

3 Figure 3. Upper panel shows the raw data and bottom panel shows the filtered data. Diurnal
 4 variations of SVO (grey) and LABS, west Pasadena (red) and Santa Anita Park (blue), XCO₂ and
 5 XCH₄ from around 8:30 to 16:30 on seven consecutive days in May 2012. Error bars represent
 6 the RMS of the retrieval spectral fitting residual. Bad data points, such as data taken in the
 7 cloudy morning of May 11, were removed from the filtered data set. From May 5-9, the FTS was
 8 operated in the target mode, taking alternate measurements among SVO, west Pasadena and
 9 Santa Anita Park. On May 10-11, standard measurement cycle was performed, resulting in fewer
 10 measurements from each target.

11

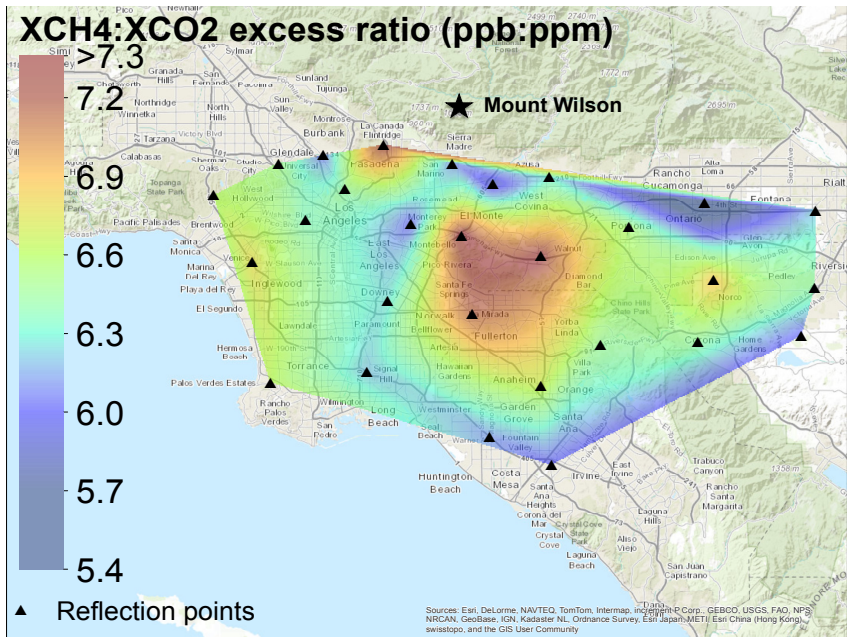
12



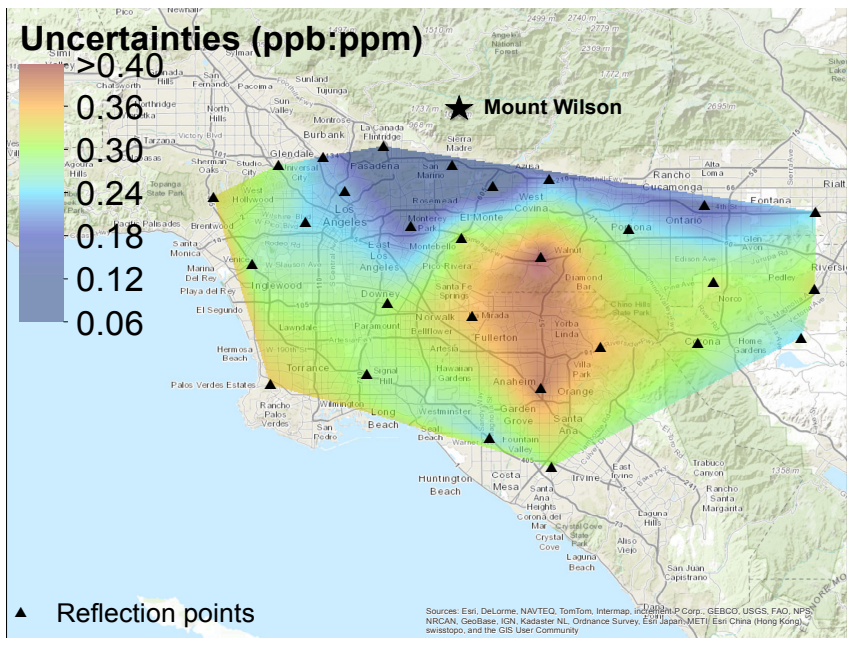
1
 2 Figure 4. Correlations between XCH_{4(XS)} (ppb) and XCO_{2(XS)} (ppm) for west Pasadena and Santa
 3 Anita Park between the period of September 2011 and October 2013.

4

5



1



2

3 **Figure 5.** Maps of correlation slopes of XCH₄(X_{CS}):XC₀₂(X_{CS}) (top) and their uncertainties (one
 4 standard deviation) (bottom) in the Los Angeles megacity observed by the CLARS-FTS between
 5 the period of September 2011 and October 2013.

6